Journal of Alloys and Compounds 509 (2011) 3963–3966

Contents lists available at ScienceDirect

Journal of Alloys and Compounds

journal homepage: www.elsevier.com/locate/jallcom

Structural and electronic properties of Si nanocrystals embedded in amorphous SiC matrix

Chao Song [a,b], Yunjun Rui [a], Quanbiao Wang [a], Jun Xu [a,*], Wei Li [a], Kunji Chen [a], Yuhua Zuo [c], Qiming Wang [c]

[a] Nanjing National Laboratory of Microstructures and School of Electronic Science and Engineering, Nanjing University, Nanjing 210093, China
[b] Department of Physics and Electrical Engineering, Hanshan Normal University, Chaozhou 521041, China
[c] State Key Laboratory on Integrated Optoelectronics, Institute of Semiconductors, Chinese Academy of Sciences, Beijing 100083, China

ARTICLE INFO

Article history:
Received 17 October 2010
Received in revised form
22 December 2010
Accepted 22 December 2010
Available online 4 January 2011

PACS:
81.15.Gh
81.40.Ef
81.40.Rs

Keywords:
Silicon carbide
Thin films
Crystal structure
Electronic properties

ABSTRACT

Si-rich hydrogenated amorphous silicon carbide thin films were prepared by plasma-enhanced chemical vapor deposition technique. As-deposited films were subsequently annealed at 900 °C and 1000 °C to form Si nanocrystals embedded in amorphous SiC matrix. Raman spectra demonstrate the formation of Si nanocrystals with size around 7–9 nm. For the sample annealed at 1000 °C, the crystallinity can be reached to 70%. As increasing the annealing temperature, the dark conductivity is increased accompanying with the increase of crystallinity of the film. The dark conductivity reaches to 1.2×10^{-6} S cm^{-1} for the sample annealed at 1000 °C, which is 4 orders of magnitude higher than that of as-deposited film. It is found that the carrier transport process is dominated by the thermally activated transport process according to the temperature-dependent conductivity results.

© 2011 Elsevier B.V. All rights reserved.

1. Introduction

Recently, the films consisting of nanocrystalline silicon (nc-Si) in amorphous SiC matrix have attracted much attention because of the unique properties of nc-Si films and their potential applications in optoelectronic devices [1–3]. By controlling the nc-Si size, spacing and the surrounding dielectric materials (SiO_2, SiC, SiN, etc.), the optical properties and carrier transport behaviors can be modified, which is helpful for optimizing the device performance. Compared with Si nanocrystals embedded in oxide and nitride matrix, the barrier height between Si nanocrystals and amorphous SiC matrix is lower, which can enhance the tunneling probability and carrier transport process [4]. Therefore, the Si nanocrystals in SiC matrix are proposed to be a suitable candidate material for the third-generation photovoltaic and other devices [5]. So far, a few reports have been published to study the structures and optical properties of nc-Si/SiC system. For example, Song et al. [3,5] have studied the effect of annealing on microstructural properties of nc-Si/SiC structures prepared by magnetron co-sputtering. The optical and electrical properties of nc-Si/SiC multilayers have also been investigated and the tunable photoluminescence was found by controlling the dot size [6,7]. In order to further improve the device performance, it is crucial to understand the electronic properties of Si nanocrystals embedded in amorphous SiC matrix together with the microstructures and optical properties.

In our previous work, we have studied the microstructures and optical properties of hydrogenated amorphous SiC (a-SiC:H) films prepared in plasma enhanced chemical vapor deposition system [8,9]. It was found that the optical properties were strongly influenced by the microstructures and chemical bonding configurations. In this paper, we prepared the Si-rich hydrogenated amorphous silicon carbide (a-$Si_{1-x}C_x$:H) thin films in plasma enhanced chemical vapor deposition (PECVD) system. The films were subsequently annealed at 900 °C and 1000 °C to get Si nanocrystals embedded in amorphous SiC matrix. The changes of microstructures were systematically investigated by various techniques. Moreover, the optical and electronic properties of Si nanocrystals embedded in amorphous SiC matrix were discussed aimed to understand the carrier transport behaviors.

* Corresponding author. Tel.: +86 2583594836; fax: +86 2583595535.
E-mail address: junxu@nju.edu.cn (J. Xu).

0925-8388/$ – see front matter © 2011 Elsevier B.V. All rights reserved.
doi:10.1016/j.jallcom.2010.12.191

2. Experimental

Hydrogenated amorphous silicon carbide thin films were prepared by PECVD technique with a gas mixture of silane (SiH_4) and methane (CH_4). The gas flow rate of SiH_4 and CH_4 was kept at 5 and 2.5 sccm. During the growth process, the r.f. power, chamber pressure and substrate temperature were 30 W, 10 mTorr and 250 °C, respectively. After deposition, the samples were dehydrogenated at 450 °C for 1 h and subsequently annealed in the conventional furnace at the temperature of 900 °C and 1000 °C for 1 h in nitrogen ambient. Quartz plates, monocrystalline Si wafers were used as substrates for various measurements.

Raman (Jobin Yvon Horiba HR800 spectrometer) and Fourier-transform infrared (FT-IR) spectroscopy (Nexus 870) were used to evaluate the structural changes and bonding configurations of samples before and after annealing. The film composition was determined by using X-ray photoelectron spectroscopy (XPS, Thermo ESCALAB 250). By integrating the C 1s peak (~283 eV) and the Si 2p peak (~100 eV), one can estimate the composition ratio of Si/C for as-deposited films is 10.8, which implies that the as-deposited samples are Si-rich amorphous SiC films.

The optical absorption of the films was measured at room temperature by Shimadzu UV-3600 spectrophotometer. Temperature-dependent dark conductivity was measured with coplanar configurations by using a pair of Al electrodes. The temperature-dependent dark conductivity of the samples was measured using a Keithley 610C electrometer and the activation energy was deduced from an Arrhenius plot. The measurement temperature is in a range of room temperature to 423 K.

3. Results and discussion

The bonding configurations of samples before and after annealing were characterized by FT-IR spectra. Fig. 1 shows the FT-IR spectra of the as-deposited sample and samples annealed at 900 and 1000 °C. As shown in Fig. 1, the wagging mode of the silicon hydride (SiH_n) at 640 cm^{-1}, the stretching mode of Si–C at 770 cm^{-1} and the stretching mode of (H–Si)–Si_3 at 2000 cm^{-1} can be clearly identified in the spectra of as-deposited samples. Meanwhile, as shown in the inset of Fig. 1, the stretching mode of C–H_n in the range of 2850–3000 cm^{-1} can be observed for the as-deposited sample. With increasing the annealing temperature, the intensity of the Si–C absorption band becomes stronger while the absorption bands at 640 cm^{-1}, 2000 cm^{-1} and the range of 2850–3000 cm^{-1} are completely disappeared due to the hydrogen effusion. Meanwhile, the peak position of Si–C bond shifts from 770 to 820 cm^{-1} as the annealing temperature increasing to 1000 °C.

Quantitatively, the concentration of Si–C bond (N_{Si-C}) can be estimated by using the integrated FT-IR absorption peak according to the following equation [10]:

$$N_{Si-C} = A \int \frac{\alpha(\omega)}{\omega} d\omega \quad (1)$$

where $\alpha(\omega)$ is the absorption coefficient, ω is the vibration frequency of the corresponding absorption band, and A is a constant related to the absorption cross section of the vibration mode. For the stretching vibration mode of Si–C bond, A is 2.13×10^{19} cm^{-2}. We can calculate the Si–C bond density according to the FT-IR spectra,

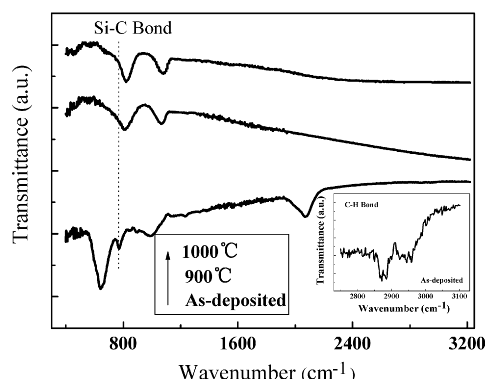

Fig. 1. FT-IR spectra of the as-deposited and annealed samples.

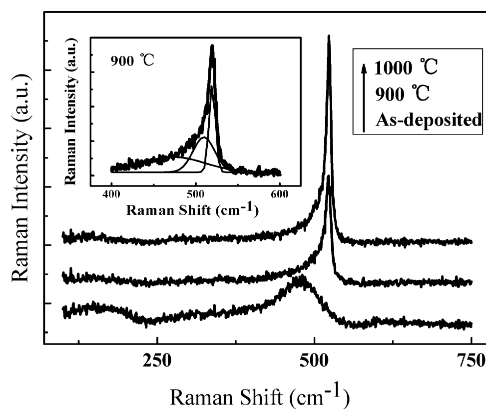

Fig. 2. Raman spectra of as-deposited sample and samples annealed at different temperatures. The inset presents the deconvolution of the Raman spectrum.

which is 2.3×10^{21} cm^{-3}, 7.8×10^{21} cm^{-3} and 1.3×10^{22} cm^{-3} for the as-deposited sample and the corresponding samples annealed at 900 °C and 1000 °C, respectively. The experimental results indicate that the Si–H and C–H bonds were broken during the annealing process and the residual Si and C atoms rearranged to form Si–C bonds which results in the increasing of Si–C bond intensity as well as the blue-shift of the Si–C bond position in FT-IR spectra [11].

Fig. 2 gives the Raman spectra of the samples annealed at different temperatures. The signals around 480 cm^{-1} and 520 cm^{-1} represent the transverse-optical (TO) mode of amorphous silicon and crystallized silicon, respectively. It is indicated that the as-deposited sample exhibits a purely amorphous structures and the crystallized Si was obtained after annealing at 900 °C and 1000 °C. In order to further study the microstructures of annealed samples, Gaussian deconvolution of the Raman spectra was performed. Three typical components corresponding to a broad band at ~80 cm^{-1}, a narrow band near 520 cm^{-1}, and an intermediate one around 510 cm^{-1} can be obtained as shown in the inset of Fig. 2. According to the empirical formula [12], it can be estimated that the average size of crystallized Si is about 7 nm and 9 nm for 900 °C and 1000 °C annealed films, respectively. The intermediate component can be attributed to the thermodynamically stable crystals with very small size [13]. It is indicated that the nc-Si can be formed in SiC matrix after thermal annealing. The volume fraction of crystallized component (X_c) can also be estimated based on Raman spectra by integrating the three Gaussian peaks [14]. It is found that the crystallized fraction X_c is about 61% for the sample annealed at 900 °C and increased to 70% after 1000 °C annealing. It is also found that the Raman bandwidth related to the crystallized Si becomes narrower for 1000 °C annealed sample compared to 900 °C annealed one. It is implied that the high annealing temperature can promote the crystallization of silicon and structural relaxation to improve the order in the crystallized phase.

Based on the XPS, FT-IR and Raman results, it can be summarized that the as-deposited sample is amorphous film containing Si–Si, Si–H and Si–C bonds. After annealing, the Si–H and C–H bonds are broken and hydrogen atoms are completely effused from the samples. The remaining Si and C atoms are rearranged to form Si–C bonds. Since the as-deposited sample is Si-rich film, the Si atoms can be precipitated and aggregated to form crystallized Si dots in the nanometer scale.

It is found that the optical band gap E_g is changed for annealed films compared to the as-deposited one due to the different film structures. The optical band gap reported here was deduced by using Tauc plot, which was usually used to describe the light absorption in amorphous and nanocrystalline semiconductor films [15,16]. Fig. 3 shows Tauc's plot of $(\alpha h\nu)^{1/2}$ versus photon energy $h\nu$

Table 1
Characteristic parameters of as-deposited and annealed samples.

Sample	Optical band gap, E_g (eV)	Conductivity activation energy, E_a (eV)	Room temperature dark conductivity, σ (S cm^{-1})
As-deposited sample	1.9	0.78	1.9×10^{-10}
900 °C annealed sample	2.0	0.49	6.3×10^{-7}
1000 °C annealed sample	2.2	0.54	1.2×10^{-6}

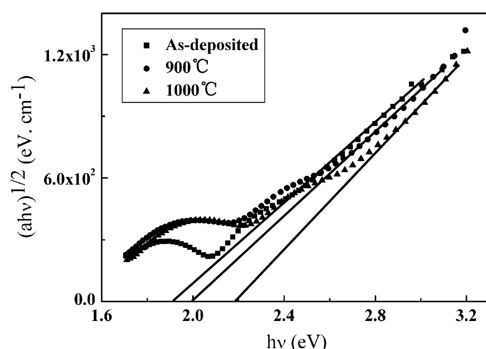

Fig. 3. The Tauc plots of the samples.

for all the samples. The calculated values of E_g are given in Table 1. It can be seen that the optical band gap E_g is 1.9 eV for the as-deposited film which represents the band gap of amorphous SiC film. After annealing, the E_g is obviously increased and reaches to 2.2 eV for the sample annealed at 1000 °C. It seems that the optical band gap after annealing is still determined by the amorphous SiC matrix instead of the nc-Si since the estimated optical band gap is far from the value of nc-Si even considering the quantum size effect. The enlargement of optical band gap for annealed films can be ascribed to the increment of Si–C bonds as discussed before. The similar phenomena were also reported previously that the band gap caused by nc-Si quantum confinement was masked by the a-SiC matrix absorption features [3].

It is interesting to investigate the electronic behaviors of samples before and after annealing. Fig. 4 gives the temperature-dependent conductivity of the as-deposited sample and the corresponding samples annealed at 900 °C and 1000 °C. The results are well agreement with the Arrhenius plots $\sigma = \sigma_0 \exp(-E_a/k_B T)$, where σ_0 is the conductivity prefactor, k_B is the Boltzmann's constant and E_a is the conductivity activation energy. The conductivity activation energy E_a of the samples can be obtained from the slope of $\ln \sigma$ versus $1/T$ curve. The room temperature dark conductivity for as-deposited sample is in the order of 10^{-10} S cm^{-1} as shown in Table 1. As the increase of annealing temperature, the room temperature dark conductivity gradually increases. When the annealing temperature increases to 1000 °C, the conductivity

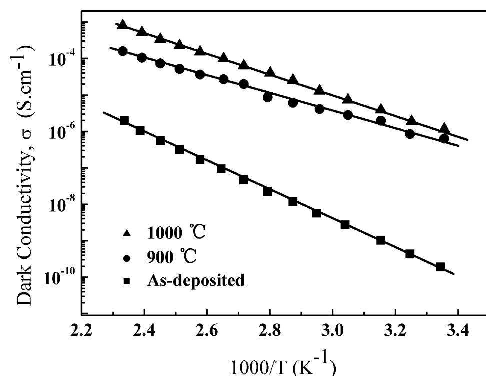

Fig. 4. Temperature-dependent conductivity of the as-deposited sample and the samples annealed at 900 °C and 1000 °C.

reaches to 1.2×10^{-6} S cm^{-1}, which is four orders of magnitude higher than that of the as-deposited film. The corresponding conductivity activation energy is 0.78 eV, 0.49 eV and 0.54 eV for the as-deposited sample and the corresponding sample annealed at 900 and 1000 °C, respectively.

As shown in Fig. 4, the linear behaviors of conductivity versus 1/T in the whole measurement temperature range for all samples suggest that the thermally activated conduction mechanism dominate the carrier transport processes [17,18]. For the as-deposited film, the extended state conduction as usually described in the amorphous semiconductors can explain the low conductivity of the a-SiC:H films. Compared with the optical band gap (1.9 eV), the small active energy indicates that the Fermi level is shifted from the middle of the gap due to the existence of the band tail states associated with the amorphous structures. After annealing at 900 °C, the dark conductivity is obviously increased, which can be attributed to the formation of nc-Si in the amorphous SiC host matrix. The crystallized Si nanocrystals, which have the small band gap compared with the amorphous SiC film, cause the increase of the carrier density and the enhanced mobility. Consequently, the dark conductivity is significantly enhanced compared to the as-deposited film. Annealing at 1000 °C further promotes the crystallization and causes the conductivity increase to 1.2×10^{-6} S cm^{-1}. Meanwhile, the conductivity activation energy for annealed films represents the energy difference between the bottom of conduction band and the Fermi level in the nc-Si. Since the average size of nc-Si in our cause is 7–9 nm, the band gap is roughly estimated at 1.3 eV [19]. Therefore, the measurement results indicate that the Fermi level is located at the midgap. With increasing the annealing temperature to 1000 °C, the increase in conductivity activation energy reflects the improved crystallinity and structural order which shifts the Fermi level to the midgap.

4. Conclusion

Si-rich a-$Si_{1-x}C_x$:H thin films were deposited by plasma-enhanced chemical vapor deposition technique. nc-Si embedded in amorphous SiC matrix was formed by thermal annealing at 900 °C and 1000 °C. For the sample annealed at 1000 °C, the average sizes of Si nanocrystals are about 9 nm, and the crystallinity can be reached as high as 70%. The optical band gap is determined by the amorphous SiC matrix which is increased from 1.9 to 2.2 eV as increasing the annealing temperature, due to the increase of the Si–C bonds after annealing. Electronic measurements show that the dark conductivity can be as high as 1.2×10^{-6} S cm^{-1} for 1000 °C annealed film due to the formation of nc-Si, which is four orders of magnitude higher than that of as-deposited sample. The electronic transport of annealed films was dominated by the thermally activation process and high annealing temperature is helpful for relaxing the film structures as indicated by the high conductivity and activation energy.

Acknowledgements

The work is supported by "973" project (No. 2007CB613401) and NSF of China (Nos. 61036001 and 10874070) and NSF of Jiangsu Province (BK2010010).

References

[1] L.F. Marsal, J. Pallares, X. Correig, J. Appl. Phys. 85 (1999) 1216.
[2] J. Xu, L. Yang, Y.J. Rui, J.X. Mei, X. Zhang, W. Li, Z.Y. Ma, L. Xu, X.F. Huang, K.J. Chen, Solid State Commun. 133 (2005) 565.
[3] D. Song, E.–C. Cho, G. Conibeer, Y.–H. Cho, Y. Huang, S. Huang, C. Flynn, M.A. Green, J. Vac. Sci. Technol. B 25 (2007) 1327.
[4] C.-W. Jiang, M.A. Green, J. Appl. Phys. 99 (2006) 114902.
[5] D. Song, E.–C. Cho, G. Conibeer, C. Flynn, Y. Huang, M.A. Green, Sol. Energy. Mater. Sol. Cells 92 (2008) 474.
[6] Y. Kurokawa, S. Tomita, S. Miyajima, A. Yamada, M. Konagai, Jpn. J. Appl. Phys. 46 (2007) L833.
[7] Y. Kurokawa, S. Yamada, S. Miyajima, A. Yamada, M. Konagai, Curr. Appl. Phys. 10 (2010) S435.
[8] L. Wang, J. Xu, T.F. Ma, W. Li, X.F. Huang, K.J. Chen, J. Alloys Compd. 290 (1999) 273.
[9] J. Xu, J.X. Mei, Y.J. Rui, D.Y. Chen, Z.H. Cen, W. Li, Z.Y. Ma, L. Xu, X.F. Huang, K.J. Chen, J. Non-Cryst. Solids 352 (2006) 1398.
[10] A.R. Oliveira, M.N.P. Carreño, J. Non-Cryst. Solids 352 (2006) 1392.
[11] W.K. Choi, T.Y. Ong, L.S. Tan, F.C. Loh, K.L. Tan, J. Appl. Phys. 83 (1998) 4968.
[12] E. Edelberg, S. Bergh, R. Naone, M. Hall, E.S. Aydi, J. Appl. Phys. 81 (1997) 2410.
[13] D. Das, K. Bhattacharya, J. Appl. Phys. 100 (2006) 103701.
[14] A.T. Vautsas, M.K. Hatalis, J.B. Boyce, A. Chiang, J. Appl. Phys. 78 (1995) 6999.
[15] X.J. Hao, E.-C. Cho, C. Flynn, Y.S. Shen, G. Conibeer, M.A. Green, Nanotechnology 19 (2008) 424019.
[16] S. Mirabella, R. Agosta, G. Franzò, I. Crupi, M. Miritello, R. Lo Savio, M.A. Di Stefano, S. Di Marco, F. Simone, A. Terrasi, J. Appl. Phys. 106 (2009) 103505.
[17] C. Song, G.R. Chen, J. Xu, T. Wang, H.C. Sun, Y. Liu, W. Li, Z.Y. Ma, L. Xu, X.F. Huang, K.J. Chen, J. Appl. Phys. 105 (2009) 054901.
[18] S.Y. Myong, K.S. Lim, M. Konagai, Appl. Phys. Lett. 88 (2006) 103120.
[19] T.-Y. Kim, N.-M. Park, K.-H. Kim, G.Y. Sung, Y.-W. Ok, T.-Y. Seong, C.-J. Choi, Appl. Phys. Lett. 86 (2004) 5355.